High-confinement-mode edge stability of Alcator C-mod plasmas

D. A. Mossessian, P. Snyder, A. Hubbard, J. W. Hughes, M. Greenwald et al.

Citation: Phys. Plasmas **10**, 1720 (2003); doi: 10.1063/1.1561618
View online: http://dx.doi.org/10.1063/1.1561618
View Table of Contents: http://pop.aip.org/resource/1/PHPAEN/v10/i5
Published by the American Institute of Physics.

High-confinement-mode edge stability of Alcator C-mod plasmas[a)]

D. A. Mossessian[b)]
MIT, Plasma Science and Fusion Center, Cambridge, Massachusetts 02139

P. Snyder
General Atomics, P.O. Box 85608, San Diego, California 92186

A. Hubbard, J. W. Hughes, M. Greenwald, B. LaBombard, J. A. Snipes, and S. Wolfe
MIT, Plasma Science and Fusion Center, Cambridge, Massachusetts 02139

H. Wilson
EURATOM/UKAEA Fusion Association, Culham Science Centre, Abingdon, Oxon, OX14 3DB, United Kingdom

(Received 12 November 2002; accepted 27 January 2003)

For steady state high-confinement-mode (H-mode) operation, a relaxation mechanism is required to limit build-up of the edge gradient and impurity content. Alcator C-Mod [Hutchinson *et al.*, Phys. Plasmas **1**, 1511 (1994)] sees two such mechanisms—EDA (enhanced D-alpha H mode) and grassy ELMs (edge localized modes), but not large type I ELMs. In EDA the edge relaxation is provided by an edge localized quasicoherent (QC) electromagnetic mode that exists at moderate pedestal temperature $T<500$ eV, high pedestal density, and high edge safety factor, $q_{95}>3.5$, and does not limit the buildup of the edge pressure gradient. The q boundary of the operational space of the mode depends on plasma shape, with the q_{95} limit moving down with increasing plasma triangularity. At high edge pressure gradients and temperatures the mode is replaced by broadband fluctuations ($f<50$ kHz) and small irregular ELMs are observed. Ideal MHD (magnetohydrodynamic) stability analysis that includes both pressure and current driven edge modes shows that the discharges where the QC mode is observed are stable. The ELMs are identified as medium n ($10<n<50$) coupled peeling/ballooning modes. The predicted stability boundary of the modes as a function of pedestal current and pressure gradient is reproduced in experimental observations. The measured dependence of the ELMs' threshold and amplitude on plasma triangularity is consistent with the results of ideal MHD analysis performed with the linear stability code ELITE [Wilson *et al.*, Phys. Plasmas **9**, 1277 (2002)]. © *2003 American Institute of Physics.* [DOI: 10.1063/1.1561618]

I. INTRODUCTION

Formation of an edge transport barrier in high confinement mode (H mode) of tokamaks' operation is accompanied by a buildup of strong temperature and density gradients in a narrow region of the plasma in the vicinity of the separatrix (pedestal region). It has been shown, for example, in Refs. 1–3, that total confinement and core transport are directly linked to the height and gradient of the temperature and pressure pedestal. When these gradients become sufficiently strong, they drive edge MHD (magnetohydrodynamic) instabilities that limit further pedestal growth. The most common type of such instabilities are edge localized modes (ELMs)—short bursts of transport that intermittently relax the pedestal gradients and provide steady state operation of H-mode discharges.[4] Large type I ELMs, which are the major edge relaxation mechanism on most of the existing tokamaks, drive considerable particle and energy fluxes that present a significant power load on the divertor target plates. On Alcator C-Mod, however, type I ELMs have never been observed. Instead more benign instabilities appear to drive enhanced particle transport at the edge of H-mode plasmas, leading to steady state operation. We present the results of recent experimental and numerical studies of these edge instabilities on Alcator C-Mod.[5]

The most extensively studied edge instability is a quasicoherent (QC) electromagnetic mode ($f=50$–150 kHz), localized in the outer part of the pedestal that appears to drive enhanced particle transport in enhanced D-alpha (EDA) H mode.[6–8] It is established experimentally that the QC mode exists in a well-defined region of edge parameter space, requiring moderate pedestal temperature ($T_e^{\mathrm{ped}}<500$ eV), high pedestal density, and high edge safety factor ($q_{95}>3.5$).[9] The edge safety factor boundary appears to depend on plasma shape, with higher plasma triangularities favoring EDA operation at lower q. Ideal MHD stability analysis that includes both pressure and current driven intermediate n modes (stability code ELITE[10,11]) shows that the plasma edge is stable in typical EDA discharges. On the other hand, the nonlinear real geometry modeling based on Braginskii fluid equations (boundary turbulence code BOUT[12,13]) shows, for an EDA plasma discharge, the existence of an edge localized resistive x-point mode with characteristics (location, wave number, frequency) similar to the measured parameters of the QC mode. Based on these results the QC mode was ten-

[a)]Paper KI2 5, Bull. Am. Phys. Soc. **47**, 184 (2002).
[b)]Invited speaker. Electronic mail: mossessian@psfc.mit.edu

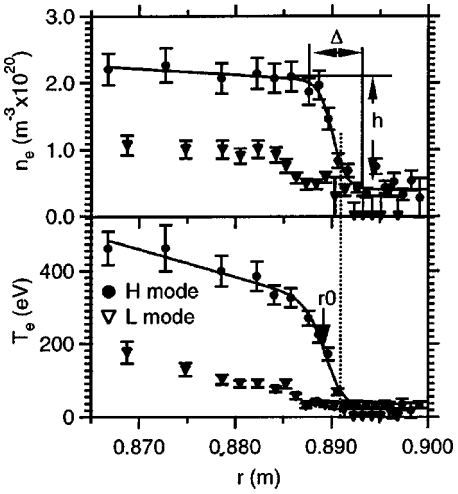

FIG. 1. Typical L and H-mode pedestal profiles measured by edge Thomson scattering. The tanh fit to the H-mode profiles are shown (solid line) together with definitions of pedestal parameters (height h, width Δ, and position $r0$).

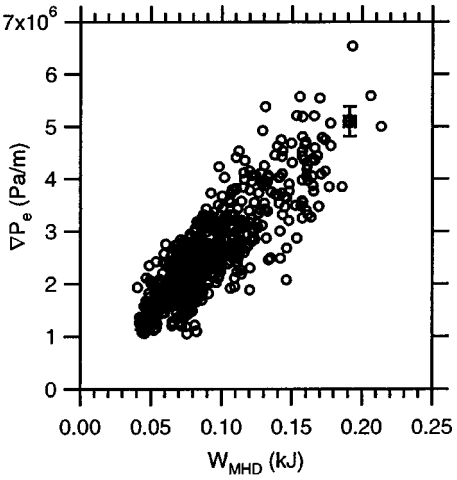

FIG. 2. Scaling of plasma stored energy with pedestal pressure gradient.

tatively identified as a resistive ballooning mode.

In high density, high input power discharges with both edge pressure gradient and edge temperature higher than in the EDA region, the QC mode is replaced by low frequency ($f<50$ kHz) broadband fluctuations. In this regime small irregular ELMs are observed with average frequency around 600 Hz. MHD stability analysis shows that these discharges are ideal ballooning stable.[9] A model was proposed that identifies the ELMs as a combination of pressure gradient driven ballooning modes and edge current driven peeling modes.[10,11] A number of ELMing, ELM-free, and EDA equilibria were analyzed using the stability code ELITE. It was found that the observed threshold for ELMs in pedestal parameter space is consistent with the coupled peeling/ballooning modes model. The model also describes in a consistent way the measured dependence of the ELMs characteristics on plasma shape.

II. PEDESTAL PARAMETERS AND H-MODE CONFINEMENT

The results presented in this paper are based mainly on a high resolution edge Thomson scattering diagnostic that is designed to map the details of temperature and density profiles to the H-mode pedestal region. The diagnostic is described in detail in Ref. 14. To parametrize the pedestal profiles the measured profiles are fitted to a hyperbolic tangent function (see Ref. 14 for details). In Fig. 1 typical pedestal H-mode profiles together with the fitted curve and the parameters used to describe the pedestal region are shown. The value of the pedestal gradient as used below in this paper represents the maximum pedestal gradient obtained from the tanh fit. The pedestal parameters routinely measured during C-Mod plasma operation are used to populate an edge database that contains also the global plasma parameters, plasma shape, and confinement characteristics. The type of H mode is defined based on the observed type of edge fluctuations (see Ref. 9 for details) measured by fluctuation diagnostics—phase contrast interferometry, reflectometer,[15] and magnetic coils. The large set of data representing different types of H modes and a wide range of plasma parameters allows us to establish correlations of pedestal parameters with plasma confinement and their scalings with global plasma parameters, leading to improved understanding of pedestal physics and mechanism of pedestal control and improvement of plasma performance.

It has been established experimentally that global confinement characteristics of an H-mode plasma are directly linked to the pedestal height and gradient.[1–3] Figure 2 shows the dependence of plasma stored energy in H mode on pressure pedestal gradient observed on Alcator C-Mod. It should be noted that since on C-Mod the pedestal width does not change significantly over the entire operational range of the H modes and was observed not to scale with major plasma parameters, similar correlation exists between pressure pedestal height and stored energy. The set of data used in Fig. 2 represents a variety of H-mode discharges with a wide range of engineering plasma parameters (plasma current, magnetic field, etc.) for various types of H mode. The observed correlation of pedestal gradient or height and plasma stored energy is essentially a result of resilience of core plasma profiles (see, for example, Ref. 16).

The measured correlation of P_e^{ped} and W_{stored} is an indication of a direct dependence of plasma confinement on pedestal characteristics. Therefore, establishing dependence of the pedestal magnitude on plasma parameters is important for understanding and optimization of the tokamak performance. The major effort in this direction has produced a number of scalings that allows us to predict pedestal parameters in a variety of operational regimes on C-Mod.[17] In Fig. 3 one such scaling is presented, showing dependence of pressure pedestal gradient in EDA and ELM-free H modes on plasma parameters—current I_p, electron density in Ohmic phase prior to the L-H transition $n_{L,0}$, and power flowing across the separatrix P_{SOL}:

$$\nabla P_e^{\mathrm{ped}} \propto I_p^{1.98\pm0.11} \cdot P_{\mathrm{SOL}}^{0.48\pm0.06} \cdot n_{L,0}^{-0.56\pm0.05}. \quad (1)$$

The scaling was obtained using multivariable regression on a large set of plasma parameters. The result can be under-

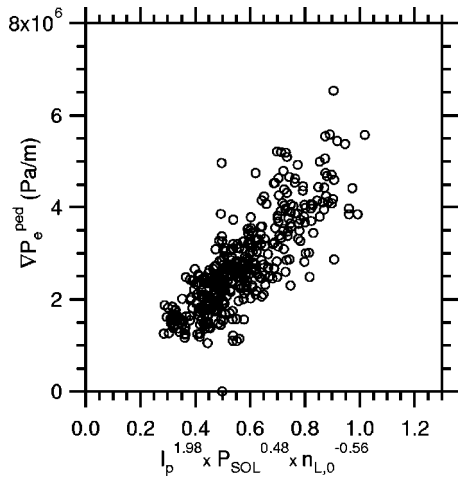

FIG. 3. Scaling of pedestal pressure gradient with plasma parameters obtained with multivariable regression fit.

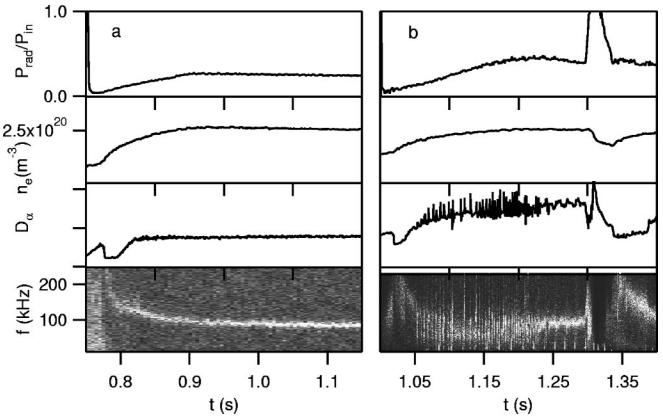

FIG. 4. Magnetic fluctuation spectrum showing a QC mode and small ELMs together with divertor D_α signal and traces of line integral density and total radiated power fraction. In ELMing discharge the QC mode starts at ~1.04 s following L–H transition (~1.02 s) and brief ELM-free period. The mode is replaced by broadband fluctuations (ELMs) at ~1.05 s and reappears at ~1.23 s when edge temperature drops.

stood qualitatively by considering observed dependencies of the temperature and density pedestal parameters on plasma parameters. The density pedestal height on C-Mod is linearly dependent on H-mode core density, which in turn is defined by two plasma parameters—current and Ohmic target density $n_{L,0}$. No gas fueling is normally used in C-Mod during the H mode and plasma density is uniquely defined by those two parameters at a given toroidal magnetic field B_t. On the other hand, the magnitude of the temperature pedestal is set by the available heat source—power flow from the core into the scrape-off layer (SOL), defined as

$$P_{\mathrm{SOL}} = P_{\mathrm{in}} + P_{\mathrm{Ohm}} - P_{\mathrm{rad}} - \frac{dW}{dt},$$

where P_{in} is input heating power (ICRH power in C-Mod), P_{Ohm} is Ohmic heating power, P_{rad} is the total radiated power, and W is the plasma stored energy.

The I_p^2 scaling alone would indicate a ballooning character of the pedestal instabilities since in this case the ballooning parameter

$$\alpha = \frac{2\mu_0 R q^2}{B_t^2} \nabla P_e$$

is constant, which would suggest that the pedestal gradient is limited by the MHD activity. However, the dependence of pressure gradient on power flow across the separatrix indicates that pedestal growth in the EDA regime observed on C-Mod is not limited and the height of the temperature pedestal increases monotonically with increasing heating power at a constant density. On the other hand, at constant input power the temperature pedestal decreases with increasing density, which may explain the inverse dependence of the pressure pedestal on target plasma density in the scaling (1).

III. PEDESTAL PARAMETERS AND THE CHARACTER OF H MODE

The scaling (1) is inferred from a set of data that includes both EDA and ELM-free H modes. The ELM-free H mode observed on Alcator C-Mod is characterized by absence of any edge fluctuations, which leads to continuous impurity accumulation in the plasma, exponential growth of radiated power, and eventual radiative collapse of the H mode.[6] By contrast, EDA is a steady state H mode that can exist as long as auxiliary heating is applied. In EDA the enhanced impurity transport appears to be driven by a quasicoherent electromagnetic mode localized in the pedestal region. The pedestal gradient scaling indicates that the QC mode, although apparently affecting the particle transport across the separatrix, does not limit the growth of pedestal pressure gradient. Recent experiments and stability analysis on Alcator C-Mod have shown that continuously increasing heating power leads to the growth of the pedestal pressure gradient to the values that exceed by more than a factor of 2 the ideal ballooning stability limit calculated without taking into account the stabilizing effect of edge bootstrap current.[9] It was found that at highest values of edge pressure gradient and temperature achievable to date in Alcator C-Mod $[\nabla P_{\mathrm{ped}} \geqslant 1.10^7$ Pa/(Wb/rad)] the QC mode is replaced by broadband fluctuations and small ELMs are observed.

In Fig. 4 the magnetic fluctuation spectrum of both the QC mode and ELMs together with traces of total radiated power normalized to the input heating power, line average density, and D_α radiation are shown for a pure EDA H mode [Fig. 4(a)] and a discharge with ELMs [Fig. 4(b)]. In an EDA discharge the QC mode is clearly seen in the fluctuation spectrum obtained by a magnetic coil installed on a tip of the scanning probe that dwells near the plasma separatrix. In the ELMy discharge, as in a regular EDA, the QC mode with ramping down frequency appears after a brief ELM-free period [1.02–1.04 s, Fig. 2(b)]. The mode is replaced by ELMs (1.05 s) when the pedestal temperature grows above 400 eV and reappears (1.23 s) when the edge cools down because of increasing radiated power fraction. In this example the H mode is terminated by a large impurity injection seen in the radiated power trace. It has been shown previously[9,6,7] that the QC mode, which is characteristic for EDA regime, exists in a well-defined edge parameter space. Generally, the mode requires high values of edge q (q_{95} above 3.5) and moderate

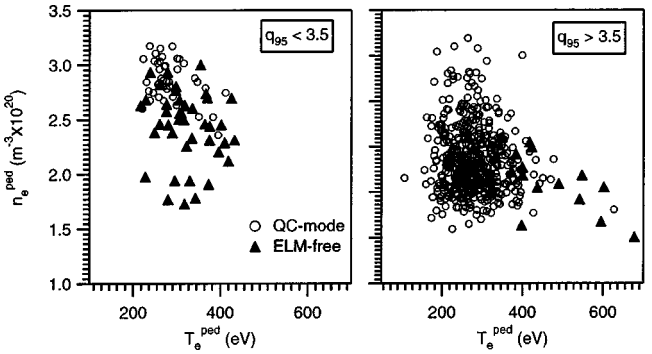

FIG. 5. Operational boundary of QC mode is pedestal temperature (T_e^{ped}), density (n_e^{ped}), and edge q space.

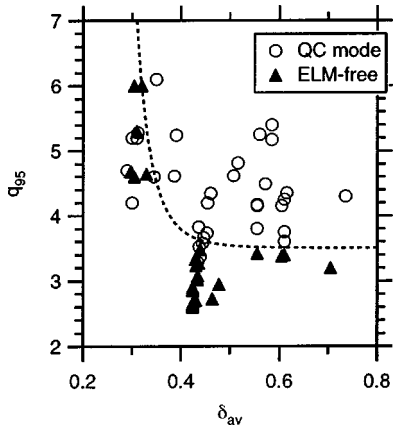

FIG. 6. Modification of the q_{95} boundary of QC-mode operation by plasma shape (triangularity).

values of pedestal temperature. At higher T_e^{ped} or lower q_{95} the mode is usually replaced by ELM-free regime. Recent studies show, however, that the mode's operational space cannot be uniquely described by the combination of these two parameters (q_{95} and T_e^{ped}). It is demonstrated (see Fig. 5) that the QC mode can be obtained at low q_{95} values in H modes with high pedestal density ($n_e^{\mathrm{ped}} > 3\times 10^{20}$ m^{-3}), while the temperature boundary seems to hold over the wide range of values of q.

The observed dependence of the H-mode fluctuations character on pedestal temperature and density suggests that edge collisionality may play a significant role in triggering of the QC mode. The fact that the mode exists only in plasmas with pedestal temperature below a certain threshold and at the same time requires high density and/or high q indicates that the QC mode favors highly collisional edge (neoclassical collisionality being defined as

$$\nu_e^* \propto \frac{qRn_eZ \ln \Lambda_e}{T_e^2 \epsilon^{3/2}},$$

where Λ_e is a Coulomb logarithm and ϵ is inverse aspect ratio). No clear boundary exists, however, between ELM-free (QC-mode free) operational space and QC-mode region if collisionality is considered as one of the independent variables. The dependence of the mode character on temperature, density, magnetic topology (q) and shape (see the following), together with tentative identification of the mode as a resistive ballooning x-point mode[12,13] suggests a complex multidimensional threshold for the mode triggering which is not likely to be described in terms of one or two simple variables like edge collisionality.

The q_{95} boundary of the QC mode space can also be modified by changing the shape of the plasma. Figure 6 summarizes the results of measurements of edge fluctuations in discharges of different shape and current. The QC mode is observed predominantly in discharges with high values of q_{95} in strongly shaped plasmas (with average triangularity $\delta_{\mathrm{av}} > 0.4$). As q decreases, the mode becomes weaker and eventually disappears, leading to ELM-free H mode. At low triangularity the QC mode can be achieved only for the values of q_{95} above 5. At lower q the mode frequency spectrum widens and the rising level of radiated power indicates increasing accumulation of impurities. It should be noted that the "standard" C-Mod equilibrium is up-down asymmetric and the changes of average δ_{av} are obtained in the experiments by simultaneous changes of lower and upper triangularities. It is not possible to say now whether the observed effect of plasma shape on QC mode is related to only one of the shaping parameters (δ_{lower} or δ_{upper}) or to both of them simultaneously. It is clear that no hard boundary exists between EDA and ELM-free H modes. The QC mode amplitude is changing gradually as the boundary is approached in any of the considered variables and as a consequence the character of the H mode is changing from steady state H mode with constant level of radiated power to the ELM-free H mode. Although the presence of the QC mode is generally associated with the steady state EDA regime, the mode can also be observed in some H modes with high rate of impurity accumulation and radiated power, characteristic to ELM-free regime. It appears that the amplitude of the mode should be sufficiently large to produce a steady EDA H mode. This observation is in agreement with the previously reported dependence of the effective particle diffusivity in the pedestal region on the amplitude of the QC mode.[7]

IV. SMALL ELMS AS COUPLED PEELING/ BALLOONING MODES

The ELMy regime can be achieved at high q_{95} by simultaneous increase of edge temperature and density, which leads to higher edge pressure gradient. The boundaries between EDA, ELM-free, and ELMy regimes are demonstrated in Fig. 7, where the values of T_e^{ped} and n_e^{ped} measured in the three types of H mode are plotted for values of q_{95} above 3.5 and a wide range of plasma shapes. The ELMs generally appear at higher pedestal pressure (pressure gradient) than EDA and the considerable overlap in operational regions of QC mode and ELMs can most likely be explained by a wide range of plasma shapes included in the data set in Fig. 7. The ELMs observed on C-Mod are small, irregular, high frequency bursts of edge transport (see Ref. 9 for more details) that cannot at the moment be classified as any of the known ELM types (type I, II, or III[18]) since not enough data are available to determine a dependence, if any, of their frequency and amplitude on heating power. Since the ELMs

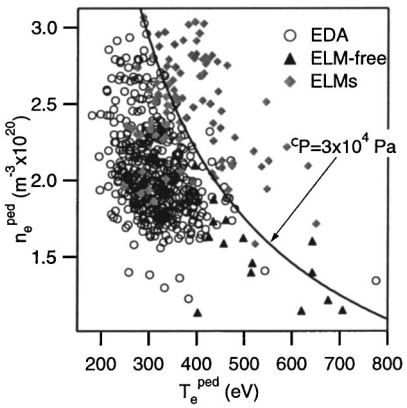

FIG. 7. Boundaries between EDA, ELM-free, and ELMy regimes in pedestal parameter space. Each point on the graph is a time point that could be identified as one of the three H-mode types by fluctuation diagnostics. ELMs appear in the high pedestal pressure region.

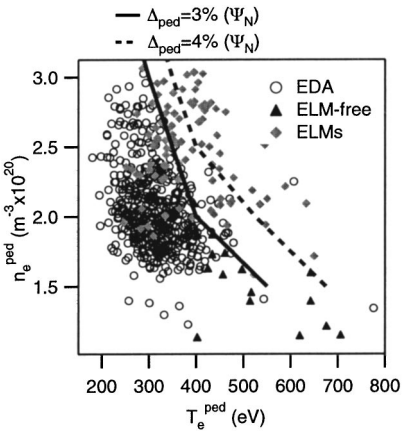

FIG. 8. Peeling/ballooning mode stability boundary calculated with ELITE for a model equilibrium with typical C-Mod parameters and different pedestal width. The modeling results are compared with the experimentally observed boundary between EDA and ELMing regimes.

appear at the values of pressure gradient higher than that of the EDA H mode and at levels of heating power two to three times above the L/H transition threshold, it is likely that they cannot be classified as type III that usually exist near the L/H threshold.

The observed small amplitude, high frequency ELMs appear to drive sufficient particle transport at the edge to achieve a quasisteady state H-mode regime without high power load on divertor plates (as opposed to low frequency, large type I ELMs) at high edge pressure gradient leading to enhanced energy confinement. Understanding physics of these ELMs is therefore important since this regime may be relevant to the future tokamak reactor operation. The observed characteristics of small ELMs are consistent with the proposed model of ELMs as intermediate *n* coupled peeling/ballooning MHD modes[10,11] driven by a combination of edge pressure gradient and edge current. The importance of the current driven term implies sensitivity of the mode stability to the edge temperature as well as pressure gradient. First results of the stability analysis performed with the linear ideal MHD stability code ELITE show that the modes become unstable at the values of $\nabla P_e^{\mathrm{ped}}$ and T_e^{ped} typical for small ELMy regimes on C-Mod.[9] The analysis has shown that the mode stability is very sensitive to the values of edge current. Since no edge current measurements exist on C-Mod, the current density was modeled using a collisional model for neoclassical resistivity and collisionality.[19] The details of the analysis and results of the sensitivity studies are described in Ref. 9.

The analysis of stability boundary for peeling/ballooning modes was performed on a model equilibrium constructed with typical C-Mod plasma parameters (toroidal field $B_t = 5.3$ T, plasma current $I_p = 1$ MA) and shape (triangularity $\delta = 0.4$, elongation $\kappa = 1.6$) using a modeled pedestal temperature and density profiles with the pedestal width $\Delta = 0.03-0.04\Psi_N$ ($\sim 4-6$ mm, which is a typical C-Mod pedestal width). The pedestal temperature was scanned at several fixed values of pedestal density over the range typical for C-Mod and the values of temperature at which first unstable modes appeared indicated the stability boundary. The results of the modeling are shown in Fig. 8 together with the measured pedestal parameters for a set of C-Mod discharges corresponding to various H-mode regimes. It is seen that although the location of the boundary is quite sensitive to the value of the pedestal width (which modifies the pressure gradient at constant $T_e^{\mathrm{ped}}, n_e^{\mathrm{ped}}$) the agreement with measured threshold for ELMs is good. It should also be noted that an up–down symmetric equilibrium was used for the analysis as opposed to an asymmetric equilibria typical for C-Mod and the data set presented in Fig. 8 include a range of plasma triangularities, although the average triangularity in these discharges is near 0.4—the value that was used in modeling.

In order to compare further the results of modeling and experiments and understand the physics of transition from EDA to ELMy regime a dedicated power and density scan experiment at fixed plasma shape and current was carried out. The stability analysis was performed on a set of equilibria derived from the EDA and ELMy discharges obtained during the scan. In Fig. 9 the measured pedestal temperatures are plotted against the

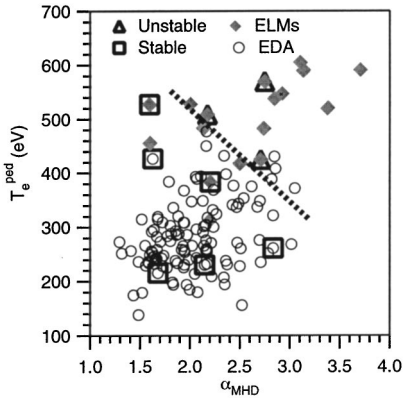

FIG. 9. Experimentally observed transition between EDA and ELMing regimes together with the results of ELITE stability analysis on a set of equilibria constructed for EDA and ELMing discharges.

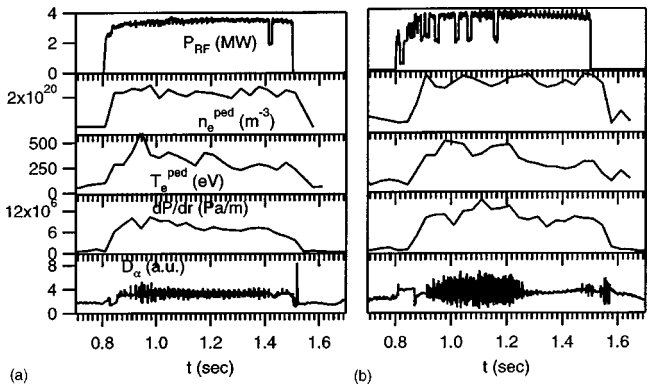

FIG. 10. Traces of input power, pedestal density, temperature and pressure gradient and D_α intensity for discharges with upper triangularity of 0.32 (a) and 0.45 (b). Increase of ELM amplitude and pedestal height and gradient is seen in higher delta discharge.

$$\alpha_{\mathrm{MHD}}=\frac{2\mu_0 R q^2 dP_e}{B_T^2}\cdot\frac{dP_e}{dr}$$

parameter, derived from edge Thomson scattering measurements. Open circles represent the points corresponding to EDA regime, closed diamonds—ELMy regimes.

A clear boundary is observed between the regimes, with ELMs appearing at values of pedestal temperature above ~500 eV and dominating in high α_{MHD} region. Nine equilibria covering the entire region of interest were constructed using EFIT equilibrium solver with pedestal pressure profiles taken for Thomson scattering measurements. In Fig. 9 large symbols mark the points that were analyzed using ELITE. The equilibria for which the peeling/ballooning modes are found to have finite growth rate are marked with triangles, the stable equilibria with squares. Within uncertainties of j_{boot} calculations and experimental measurements, ELITE shows a stability boundary consistent with measurements. The point at low α_{MHD}, high T_e^{ped} taken from an ELMing discharge is likely to be found stable by ELITE because of the uncertainties in estimates of the edge current density.

It was found experimentally that transition to the ELMy regime happens at lower input power in discharges with higher triangularity. Besides, in high triangularity plasma the ELMs have larger amplitude and pedestal temperature and pressure gradient reach higher value at lower heating power. An example of two discharges with different upper triangularities but similar values of target density and heating power is shown in Fig. 10. This observation is consistent with the model of ELMs as coupled peeling/ballooning modes. Higher triangularity should lead to higher stability boundary, which allows the pedestal to grow larger before the limiting instability is triggered. The higher values of the pedestal gradient and height lead in turn to larger growth rates of the modes, leading to larger ELMs amplitude. This is demonstrated by the ELITE analysis that was performed using equilibria from the discharges shown in Fig. 10. The stability analysis shows higher growth rates for the higher triangularity discharge.

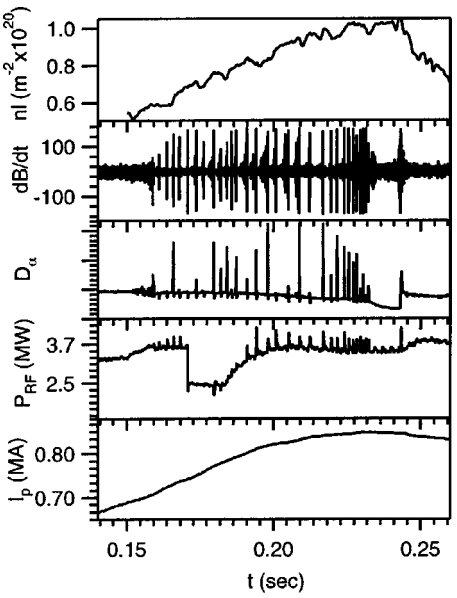

FIG. 11. ELMs driven by continuously rising plasma current in the rf induced H mode in the initial phase of the discharge. Note changing ELM frequency as the current rise rate is changing and a transition to ELM-free H mode when current rise stops.

V. ELMS TRIGGERED BY CURRENT MODULATION

General agreement of the observations of ELMing H-mode regime on C-Mod and other tokamaks[20,21] with the results of modeling of ELMs as coupled peeling/ballooning modes indicates the validity of the model for description of the edge localized modes. Since the model states that edge current plays an important role in driving the modes, one experimental verification of the model would be triggering ELMs in otherwise ELM-free H mode by a controlled variation of edge plasma current. Such an experiment was successfully carried out on COMPASS-D tokamak[22] and similar results have recently been obtained on C-Mod. Changes in edge current relative to the total plasma current are expected when plasma current is modulated on a time scale comparable to the current diffusion time. On Alcator C-Mod this scenario was realized by applying the ICRH power during the initial current ramp in the first 200 ms of discharge. In thus obtained H mode large ELMs were triggered immediately after the L/H transition. The frequency of the ELMs was increasing, and the amplitude decreasing as the rate of the current rise was slowing down, and the ELMs disappeared as soon as the plasma current reached a flattop programmed for the discharge. Figure 11 shows the traces of the line integrated density, magnetic fluctuations, D_α intensity, rf power, and plasma current for one of the discharges.

The ELMs are clearly seen on both magnetics and D_α signal. Appearance of bursts of power on rf signal synchronous with ELMs indicates that the ELMs are modifying the H-mode pedestal profiles to a considerable degree, thus improving the rf coupling to the plasma. It should be noted that the shape of the plasma is continuously evolving during the initial current rise and, since no edge current measurements are available on Alcator C-Mod, no stability analysis can be

performed on these discharges. Therefore these results can only be considered as preliminary and further experiments on current modulation at fixed plasma shape are necessary to make any definite conclusions. However, the present results can be taken as an indication that ELMs can be triggered by edge current modulation, consistent with the peeling/ballooning model that predicts appearance of ELMs if peeling modes are destabilized.

VI. CONCLUSIONS

Detailed studies of the operational boundaries of the quasicoherent mode thought to be responsible for steady state EDA H-mode behavior have been carried out. It has been shown that the boundary of the mode can be defined in multidimensional plasma parameter space (pedestal density and temperature, edge q, plasma shape) with the mode favoring highly shaped, high q, moderate temperature, high density plasmas. It has been demonstrated that MHD activity associated with the mode does not limit the growth of edge pedestal. Thus, applying high heating power (>3.5 MW) to high density H-mode plasma (with $n_e^{\mathrm{ped}} > 2\times 10^{20}\ \mathrm{m}^{-3}$) leads to formation of high ∇P_e pedestal and transition to ELMing regime with high frequency ($\sim$600 Hz) small amplitude ELMs. This steady state regime, characterized by improved energy confinement in combination with relatively benign edge MHD activity may be a prospective regime for a future burning plasma experiment. Ideal MHD stability analysis in the framework of coupled peeling/ballooning model performed using the ELITE stability code supports the conclusion that the observed ELMs are intermediate n $(10<n<60)$ peeling/ballooning modes. Modeled stability boundary for the modes is consistent with observed threshold for transition between EDA and ELMing regimes. The results of stability analysis of equilibria reconstructed from ELMing and EDA discharges are also in agreement with the observed EDA/ELMs transition. Preliminary experiments indicate that ELMs can be triggered by modulating the magnitude of the edge current relative to the total plasma current, consistent with the peeling/ballooning model that predicts appearance of ELMs if peeling modes are destabilized.

ACKNOWLEDGMENT

This work was supported by D.O.E. Coop. Agreement No. DE-FC02-99ER54512.

[1] T. H. Osborne, R. J. Groebner, L. L. Lao *et al.*, Plasma Phys. Controlled Fusion **40**, 845 (1998).
[2] M. Greenwald, R. L. Boivin, F. Bombarda *et al.*, Nucl. Fusion **37**, 793 (1997).
[3] C. S. Pitcher, A. H. Boozer, H. Murmann, J. Schweinzer, W. Suttrop, H. Salzmann, and the NBI Group, Phys. Plasmas **4**, 2577 (1997).
[4] J. W. Connor, Plasma Phys. Controlled Fusion **40**, 191 (1998).
[5] I. H. Hutchinson, R. Boivin, F. Bombarda *et al.*, Phys. Plasmas **1**, 1511 (1994).
[6] M. Greenwald, R. Boivin, P. Bonoli *et al.*, Phys. Plasmas **6**, 1943 (1999).
[7] A. E. Hubbard, R. L. Boivin, R. S. Granetz *et al.*, Phys. Plasmas **8**, 2033 (2001).
[8] J. A. Snipes, B. LaBombard, M. Greenwald *et al.*, Plasma Phys. Controlled Fusion **43**, L23 (2001).
[9] D. A. Mossessian, P. B. Snyder, M. Greenwald *et al.*, Plasma Phys. Controlled Fusion **44**, 423 (2002).
[10] H. R. Wilson, P. B. Snyder, G. T. A. Huysmans, and R. L. Miller, Phys. Plasmas **9**, 1277 (2002).
[11] P. B. Snyder, H. R. Wilson, J. R. Ferron *et al.*, Phys. Plasmas **9**, 2037 (2002).
[12] X. Q. Xu, R. H. Cohen, T. D. Rognlien, and J. R. Myra, Phys. Plasmas **7**, 1951 (2000).
[13] A. Mazurenko, M. Porkolab, D. Mossessian, J. A. Snipes, X. Q. Xu, and W. M. Nevins, Phys. Rev. Lett. **89**, 225004 (2002).
[14] J. W. Hughes, D. A. Mossessian, A. E. Hubbard *et al.*, Rev. Sci. Instrum. **72**, 1107 (2001).
[15] Y. Lin, J. Irby, P. Stek *et al.*, Rev. Sci. Instrum. **70**, 1078 (1999).
[16] W. Suttrop, M. Kaufmann, H. J. de Blank *et al.*, Plasma Phys. Controlled Fusion **39**, 2051 (1997).
[17] J. W. Hughes, D. A. Mossessian, A. E. Hubbard *et al.*, Phys. Plasmas **9**, 3019 (2002).
[18] W. Suttrop, Plasma Phys. Controlled Fusion **42**, A1 (2000).
[19] O. Sauter and C. Angioni, Phys. Plasmas **6**, 2834 (1999).
[20] L. L. Lao, Y. L. Kamada, T. Oikawa *et al.*, Proceedings of 18th IAEA Fusion Energy Conference, Sorrento, 2000.
[21] J. R. Ferron, M. S. Chu, G. L. Jackson *et al.*, Phys. Plasmas **7**, 1976 (2000).
[22] S. J. Fielding, R. J. Buttery, A. R. Field *et al.*, Proceedings of 28th EPS Conference On Controlled Fusion and Plasma Physics, Madeira, 2001.